Malaysian Journal of Civil Engineering 24(2):187-201 (2012)

TIME DEPENDENT INFLUENCE ON THE LATERAL RESPONSE OF SINGLE PILE SUBJECTED TO LATERAL LOAD

Z. H. Chik[1], J. M Abbas[2*], M. R. Taha[3], & Q. S. M. Shafiqu[4]

[1]*Associate Professor, Department of Civil and Structural Engineering, Universiti Kebangsaan Malaysia, Bangi, Selangor D H, Malaysia.*
[2] *Lecturer, Department of Civil Engineering, Diyala University, Baghuba, Iraq.*
[3]*Professor, Department of Civil and Structural Engineering, Universiti Kebangsaan Malaysia, Bangi, Selangor D H, Malaysia.*
[4]*Lecturer, Department of Civil Engineering, Nahrain University, Baghdad, Iraq.*

*Corresponding Author: *jasimalshamary@yahoo.com*

Abstract: The time dependent response of the pile foundation can be categorized as one of the effective parameters that should be taken into account during analysis and design stage. From the literatures, very few reports are available on lateral response of the pile especially on the effect of soil type. It seems to be no exact solution for laterally loaded pile foundations in consolidating elasto-plastic soil to determine the design parameter such as maximum lateral pile displacement, ultimate lateral soil resistance and *p-y* relationship. Therefore, this study investigates the effect of soil type with different intensities of loading on the lateral pile deformation and lateral soil pressure with time. Finite element analysis is carried out to evaluate the lateral pile response embedded in cohesionless and cohesive soil subjected to pure lateral load. The simulation include linear elastic model to represent the pile structural material and Mohr-Coulomb elasto-plastic model to represent the surrounding soil. Biot's equation of consolidation is used to govern the elasto-plastic material. The complete model of the whole geotechnical system are used to assess the lateral pile displacement and lateral soil pressure developed at pile face of 15m pile length and 1m pile diameter. It is shown that the lateral pile displacements increased and the lateral soil pressure was redistributed with time due to consolidation process.

Keywords: *Single pile, Consolidation, Lateral response, Axial load intensity, Finite element method.*

1.0 Introduction

Pile foundation is one of the underground structures technically affected by many geotechnical problems during the development of the Megacities. One of these problems is the time dependent behavior of the pile foundation which possibly caused by the lateral load. The lateral load usually results from the near new building or any large near civil engineering projects as well as the other normal sources of lateral load. Time dependent analysis of the structure has been limited because of complexity of the time dependent interaction between the soil and structure (Taiebat & Carter, 2001; Small & Liu, 2008). In cities where high rise buildings are close to each other, lateral load must be considered as the most important factor in the analysis and design of pile foundation.

Piles are normally designed to carry either vertical load or horizontal load. In case of piles subject to lateral loading, the failure mechanisms of short piles under lateral loads are different with long piles case (Poulos & Davis 1980). The approaches for analysis of piles are divided into two categories depending on the direction of the applied loads (Karthigeyan *et al*., 2007). First category includes the axial loaded pile, while the second category includes the analysis of pile under pure lateral load. To assess the lateral pile response, four methods are available: (a) limit state method (b) subgrade reaction method or *p*-*y* method, (c) elastic continuum method and (d) the finite element method. The brief review of historical used of the finite element technique for the analysis of lateral pile response was firstly developed by (Desai 1974, Muqtadir & Desai, 1986, Trochanis *et al*. 1991, Abbas et al. 2008 and Abbas et al. 2009).

The modelling of consolidation was studied and solved by Biot (1941). Generally essential to alternative to a numerical simulation (e. g. FEM) to solve time-dependent problems because it is complex to solve analytically. Very few examples observed to solve such problems, i.e. Carter & Booker (1984) and Taiebat & Carter (2001) analyse lateral loaded piles using two-dimensional finite element approach include efficient formula based on semi-analytical finite element method. These studies limited to predict the lateral pile response subjected to pure lateral load embedded in the cohesionless soil.

The present paper focuses on the study of time-dependent behavior of piles subjected pure lateral loads through finite-element analyses. The details of the numerical models, the finite element formulation, and results from parametric studies are discussed in the paper.

2.0 Material and Methodology

2.1 Pile Model (linear-elastic model)

This model used represents Hooke's law of isotropic linear elasticity used for modeling the stress-strain relationship of the pile material as shown in Figure 1. The model involves two elastic stiffness parameters, namely Young's modulus, E, and Poisson's ratio, ν. It is primarily used for modeling of stiff structural member for example piles in the soil (Abbas et. al 2009).

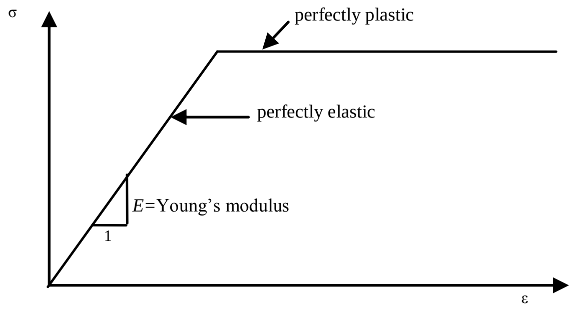

Figure 1: Stress – strain curve (Johnson et al., 2006)

According to (Abbas *et al*., 2008), the soil was modelled as Mohr-Coulomb Model. This elasto-plastic model is based on soil parameters that are known in most practical situations. The model involves two main parameters, namely the cohesion intercept, *c'* and the friction angle, *ø'*. In addition three parameters namely Young's modulus, *E'*, Poisson's ratio, *v'*, and the dilatancy angle, *ψ'* are needed to calculate the complete *σ–ε* behavior. Mohr-Coulomb's failure surface criterion is shown in Figure 2 (Potts & Zdravkovic 1999). The failure envelope as referred by Johnson *et al*. (2006) only depend on the principal stresses (σ_1, σ_3), and is independent of the intermediate principle stress (σ_2).

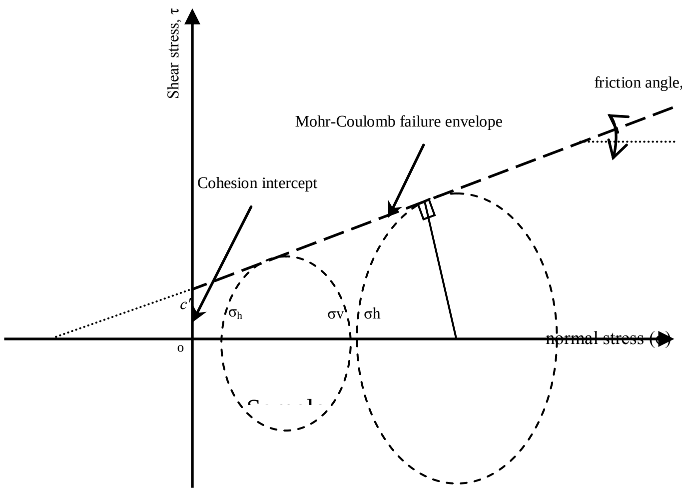

Figure 2: Mohr-Coulomb's failure surface (Potts & Zdravkovic, 1999)

Transient Formulation: An incremental formulation was used in the current work producing the matrix version of the Biot (1941) equation at the element level presented below (Smith & Griffiths 2004)

$$\begin{bmatrix} K & L \\ L^T & S+\bar{\alpha}H\Delta t_k \end{bmatrix}\begin{Bmatrix} \bar{u} \\ \bar{p} \end{Bmatrix} = \begin{bmatrix} K & L \\ L^T & S-(1-\bar{\alpha})H\Delta t_k \end{bmatrix}\begin{Bmatrix} \bar{u} \\ \bar{p} \end{Bmatrix} + \begin{Bmatrix} dF/dt+C \\ \bar{F} \end{Bmatrix} \quad (1)$$

where: K= element solid stiffness matrix, L= element coupling matrix, H= element fluid stiffness matrix, $\bar{u}$= change in nodal displacements, p change in nodal excess pore-pressures, S = the compressibility matrix, $\bar{F}$ = load vector, Δt = calculation time step, $\bar{\alpha}$ = time stepping parameter (equal to one in this work), dF/dt = change in nodal forces.

2.2 Finite Element Model

The finite element program with two-dimensional approach was developed and applied to the case of time-dependent behavior of laterally loaded single isolated piles. In order to cover all the issues of this problem, it is supported by a pre-processor to develop 2-dimensional meshes include both rectangular type prismatic elements and 8 node quadrilateral elements. The developed program has the ability to plot the 2-D mesh as illustrated in Figure 3. The pile and the surrounding soil are modelled using 8-node quadratics elements. Analysis was performed with several trail meshes with increasing refinement until the displacement did not change with more refinement. The aspect ratio of elements used in the mesh range from small closed to the pile body and when near to the pile head and base and increase refinement to wide spacing far from the pile body. All the nodes of the lateral boundary are restrained from moving in the normal direction to the respective surface representing rigid, smooth lateral boundary. The nodes at the bottom surface are restrained an all the two direction representing rough, rigid bottom surface.

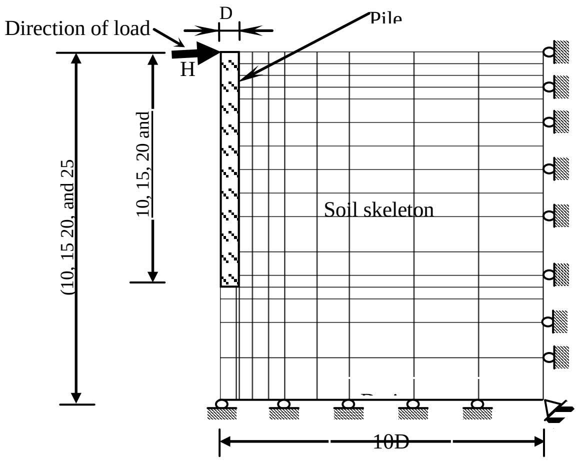

Fig. 3: 2-Dimensional finite element mesh.

2.3 Non-Dimensional Time factor

In order to examine the time dependent consolidation behaviour of the pile, it is convenient to introduce a non-dimensional time factor T, defined as (Carter & Booker 1984, Taiebat & Carter 2001, Small & Lui 2008 and Abbas et al. 2009)

$$T = \frac{c_v t}{D^2}, \text{ where} \quad (2)$$

$$, \; c_v = \frac{k(1-\upsilon_s')E_s'}{\gamma_w(1-2\upsilon_s')(1+\upsilon_s')}$$

then:

$$T = \frac{k(1-\upsilon_s')E_s' t}{\gamma_w(1-2\upsilon_s')(1+\upsilon_s')D^2} \quad (3)$$

Where the coefficient of consolidation c_v is defined in term of the permeability k, the drained modulus *E'*, and Poison's ratio *v'*, the unit weight of water γ_w and the diameter of pile *D*.

3.0 Comparison with the Existing Researches

The analysis of the behavior of a vertical pile embedded in a saturated elasto plastic soil and subjected to a lateral load was studied by Carter and Booker (1984) and Taiebat and Carter (2001) with elastic and elasto-plastic skeleton, respectively. According to Taiebat & Carter (2001) a pile studied with diameter *D* is embedded in a layer of saturated cohesionless soil which obeys the Mohr-Coulomb failure criterion. The friction angle of the soil is assumed to be ϕ' =30°. The soil is also assumed to have a submerged unit weight of γ_{sub} =0.7 γ_w, where γ_w is the unit weight of pore water, a Young's modulus for fully drained conditions given by E'_s = 3000 γ_w and a Poisson's ratio v' = 0.30. The initial value of the coefficient of lateral earth pressure is K_0= 0.5. The Young's modulus of the pile material is E_p= 1000 E'_s. The problem was analyzed by assuming elastic and elasto-plastic models for the soil. All elasto-plastic analyses have been carried out using 8-node quadrilateral finite elements on the other hand the same sequence of loading. Good comparisons were obtained between the published case results of Taiebat & Carter (2001) and the present simulation model at lateral load intensity of 15 γ_w x D^3 as shown in Fig 4. This loading was maintained constant with time and the analyses were continued, allowing excess pore pressures to dissipate, and thus for the soil to consolidate during a total time of (T=0.0001).

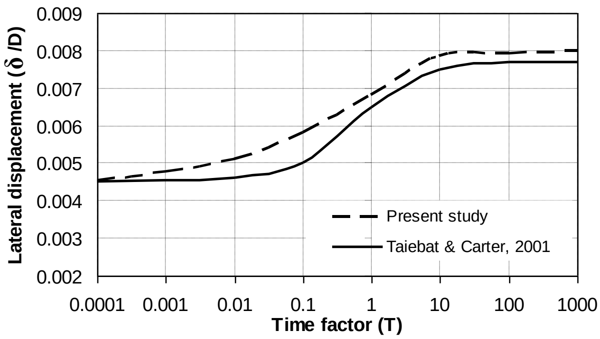

Figure 4: Comparison of the lateral displacements of the pile head in elasto-plastic soils.

The predicted load-displacement curves for the pile head, for cases where the pile deforms under fully drained state and rapid loading (i.e., undrained) conditions, are presented in Figure 5. Case is plotted for the Mohr-Coulomb soil model. The response of the pile during rapid loading is almost linear and close to the elastic response with head displacement about twice that of elastic analysis. Again good agreement was observed between present study and Taiebat & Carter (2001) results.

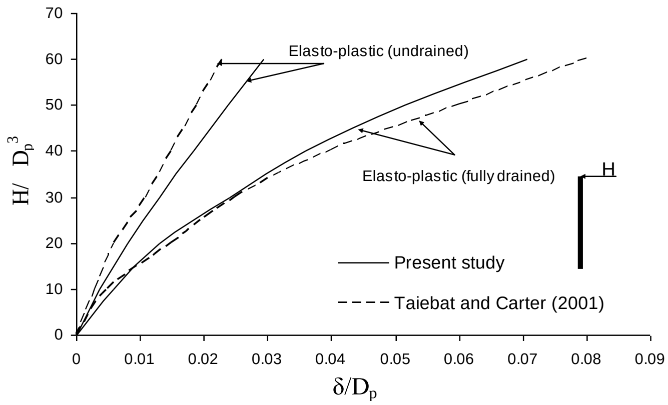

Figure 5: Lateral displacement relationships for laterally loaded piles under drained and undrained conditions

4.0 Analysis Layout

To assess all numerical analysis in this investigation using finite element program, which has the feature of modeling two-dimensional (plane strain and axisymmetric) geotechnical problems such as consolidation is developed. The finite element model of the whole geotechnical structure developed was verified based on the case study. The analysis of the behavior of a vertical pile embedded in a saturated elasto-plastic soil and subjected to a lateral load was studied by Carter & Booker 1984 and Taiebat and Carter 2001 with elastic and elasto-plastic skeleton, respectively. This study include: (1) the load intensity which taken from low value of 50 kN and increased reached to 450 kN. (2) time factor is taken from 0.0001 which means rapid load (short term) to 1.0 for long-time after loading (long term), and (3) two type of soil are considered (i.e., cohesionless and cohesive soil). The main advantage of this study is to gain new knowledge regarding the lateral pile response subjected to lateral load. The study can be referred for general case studies and also can be utilised in real situation by mobilizing the program and boundary condition according to new cases. From this simulation, we can assess the lateral pile displacement and lateral soil resistance as a function of depth, and finally can estimate *p-y* curve when designing the pile under lateral loading.

5.0 Results and Discussion

In order to analyse and design the laterally loaded pile, it is important to calculate both the maximum lateral pile displacement as well as the ultimate lateral soil resistance. In this study, the maximum lateral pile displacement was selected with time factor. In addition, the ultimate lateral soil resistance has been developed as a function of depth. Besides that, in order to understand the lateral soil distribution that help to know the position of the ultimate lateral load that take in the *p-y* design curves, this study also includes the lateral soil pressure which is developed according to depth under time dependent condition.

5.1 Development of lateral pile displacement

The lateral pile displacement that developed with depth is illustrated in Figure 6(a & b) for two types of soil. For the load intensity of ($5\gamma_w$ x D^3), small differences in the lateral settlement can be observed, whereas the lateral pile displacement increase after the increase of the load intensity to reach the maximum value of (45 γ_w x D^3). This is possibly due to dissipation of pure water pressure. In addition, the figure shows small lateral displacement in case of rapid (instantaneous) and large deformation due to consolidation (long-time). In this case, when large lateral pile displacement occurs, the lateral pile capacity reduced to minimum value with time. The main deflection of the pile occurred near to the surface with significant negative deflection appeared in the opposite pile face and below the rotation point which is between 5-7.5 D. the maximum negative deflection occurred at the toe of pile (close to pile base).

For cohesionless soil, 78.6% from the total settlement occurred during the initial stage (rapid load) and 21.4% for the long term loading. This means that when low intensity (5 γ_w x D^3) is applied, the pile is less resistant in the first stage of load and being stronger with time after dissipation of pore water pressure. While, when the pile carry large amount of loading (i.e. 45 γ_w x D^3), 29% from the total lateral settlement is carried in long term. This means that more effect of the long term loading in case of high lateral load. In the other hand, for the pile embedded on the cohesive soil, the long team settlements are measured at 16.3% and 26.8% for pile under low and high load intensities, respectively. Overall, the pile in cohesionless soil resist more in rapid load and resist less in case of long term loading.

Normally, the maximum lateral pile deflection occurred on the tip of pile and this is due to the free-headed pile. The lateral pile displacement with time at the point on pile head in both cohesionless and cohesion soil is shown in Figure 7. The figure represent different displacements with time factor (T = 0.0001 - 1.0) as well as different load magnitude. The predicted load-displacement relationship under rapid and long-time loading is presented in Figure 8(a & b) for two types of soil. These figures used to predict the lateral pile displacement according to load variation. These values limited by shadowed area for long and short time loadings.

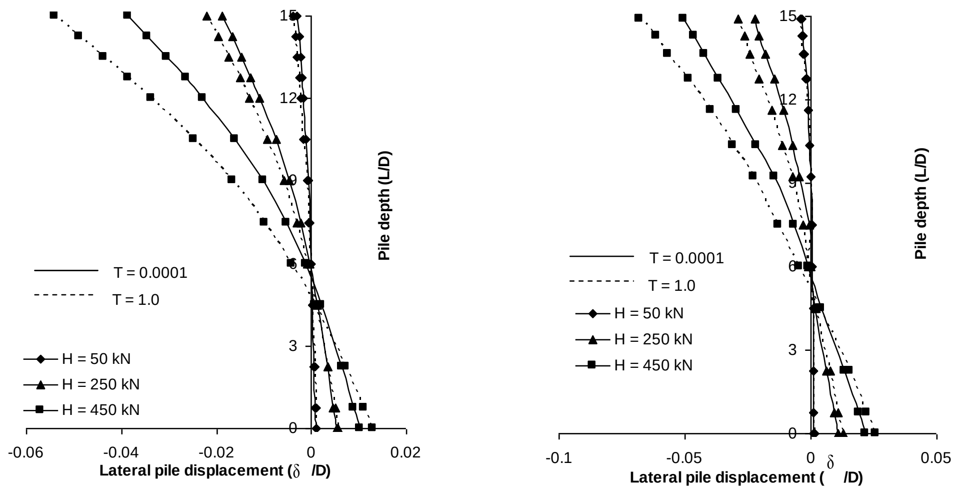

(a) (b)

Figure 6. Lateral pile displacement with depth, (a) cohesionless soil, (b) cohesive soil

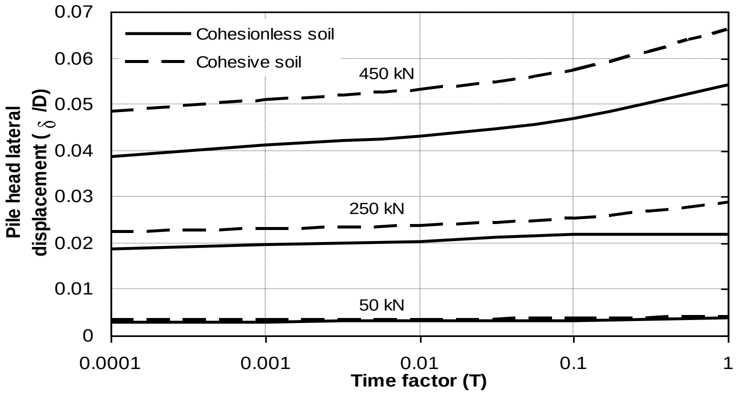

Figure 7. The predicted pile head lateral displacement with time based on three lateral loads intensities

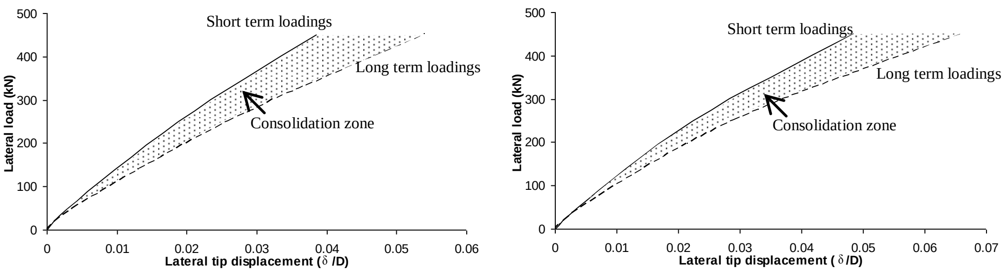

(a) (b)

Figure 8. Lateral pile displacement with depth, (a) cohesionless soil, (b) cohesive soil

The percentage of lateral displacement increment between T = 0.0001 and T = 1.0 is large for cohesionless soil which calculated using Equation (1) as below. This indicates that the pile in cohesionless soil can resist more at the rapid loading and resist less during long-time loading as compared with the pile in cohesive soil (refer Table 1). This is due to the fact that cohesionless soil has more void due to the higher permeability value compared to cohesive soils, thus in the case of rapid loading causes the pore water to carry more part of the applied load. Therefore the pore pressure increases the pile resistance by reducing the lateral displacement. However, in long term, more water dissipated causing the reduction in lateral pile resistance and results large displacement.

$$\delta_{\%} = \frac{\delta_{T=1.0} - \delta_{T=0.0001}}{\delta_{T=1.0}} \times 100 \qquad (1)$$

where:
δ% = Percentage of lateral displacement increment between T=0.0001 and T=1.0
δT=1.0 = the lateral displacement δ/D at T = 1.0 (effect of consolidation time)
δT=0,0001= the lateral displacement δ/D at T=0.0001 (rapid load)

This increment in lateral load with time is important to study and improve understanding regarding the real pile behavior with time. From this study, it can be noticed that the pile carried more than 70% of the total lateral pile capacity in the first time of loading for both type of soils. This gives indication that the pile being more risky in the first time of loading. Proposed design curve for lateral pile displacement increment with time is depicted in Figure 9. The figure include the comparison between cohesionless and cohesive soil under pure lateral load (i.e. low intensity, H=50kN, intermediate intensity, H=250kN, and high intensity, H=450kN).

Table 1: Percentage of lateral displacement increment

Load intensity (kN)	δ% (%)	
	Cohesionless soil	Cohesive soil
50	21.4	16.3
250	25.2	22.7
450	28.9	26.8

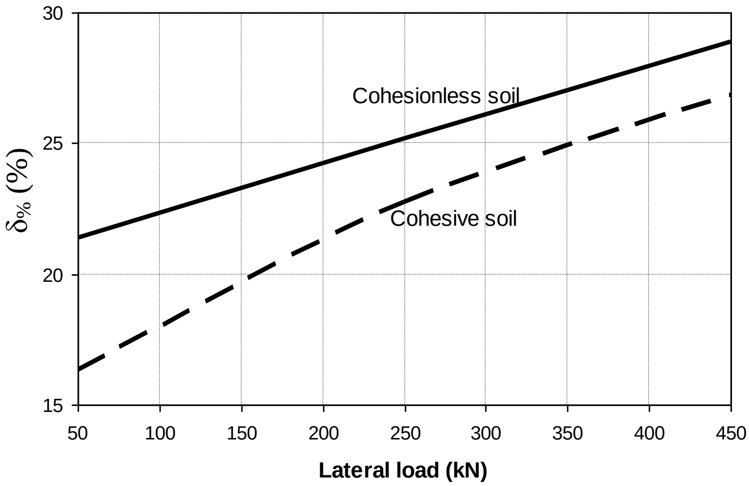

Figure 9. Lateral pile displacement increment with time fore three load intensities

5.2 Development of lateral soil resistance

Lateral soil pressures *p* in soil resulting from the lateral loads is shown in Figure 10. It can be seen that the pressure redistributed with time. Higher values of lateral pressure occurred at L/D between 1 and 3 scaled from pile head for all amount of loads. For cohesionless soil, the maximum lateral pressure occurred at L/D =2.5. In addition, at L/D=1.5 of cohesive soil case from pile tip as also recommended by Broms (1964a, b) with depth of 1.5D.

It can be seen that the load intensity is significantly affecting the front lateral load resistance distribution. The soil resistance starts from the small value near to the surface and reach the maximum in case of low loading. While in case of intermediate and high loading, we can see the maximum value occurred not on the surface. This means that the soil near surface failed due to the increment of lateral load. Hence, it is recommended to take the result from certain depth into account for design parameters. In addition, the negative lateral soil pressure occurred at the lower part of the opposite pile face. The value of the maximum negative pressure appeared at the pile toe. This values started from zero at the point of rotation and then increases to reach the maximum magnitude near the base (at pile toe) for both cases (i.e. cohesionless and cohesive soil) which also recommended by Broms (1964a,b).

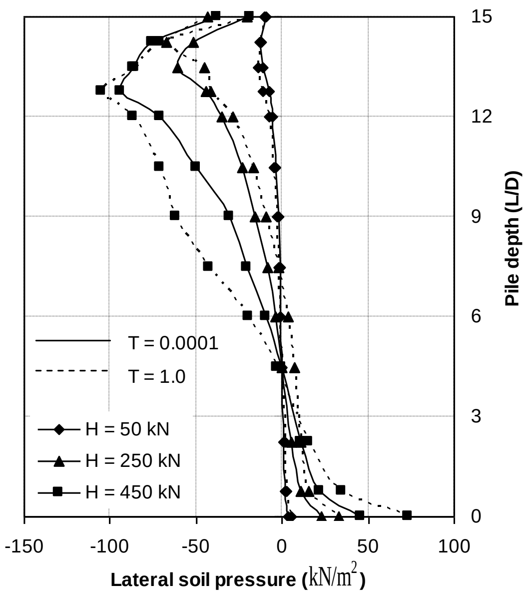

(a)

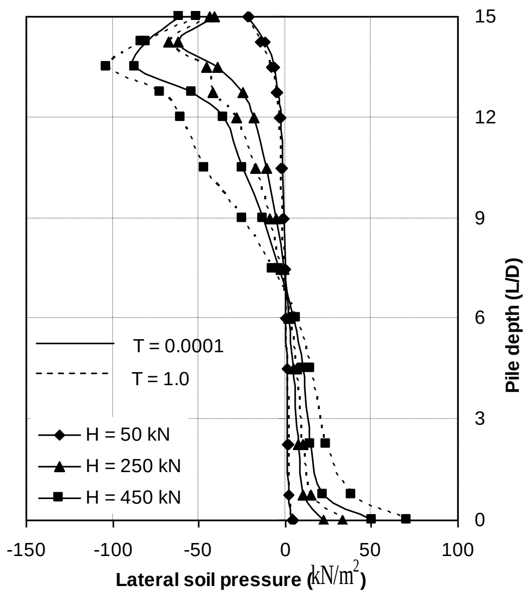

(b)

Fig 10. Lateral soil resistance with depth, (a) cohesionless soil, (b) cohesive soil

5.3 Prediction of p-y curve

The computed *p*-*y* curves at the tip of pile (at surface) and at the depth of 1.5D and 3D for pile embedded in two types of soil are shown in Figure 11. The FE results indicate that the *p*-*y* curve sensitive to the type of soil and the calculated level. Thus, this paper conducted herein supports the assumption on the effect of soil type upon *p*-*y* curve,

It can be seen that, distinct differences appeared when *p*-*y* curve was calculated based on the depth from the surface. At the point near to the surface, there is an evident of the change of the results which yielded from piles in cohesionless and cohesive soil. For the same amount of lateral settlement 10% and 20% of pile diameter, the result obtained from cohesionless soil gives lower values than the results with cohesive soil. It is may be due to early collapse of surface soil mass in case of cohesionless soil. Also it can see that the effect of time dependent factor on *p*-*y* curve, the response with cohesionless soil more sensitive with long-time loading.

Based on the prediction of *p*-*y* curve deep and close with maximum ultimate lateral soil pressure, the convergent performance of the two types of soil can be clearly observed. The long term loading is affected and at the same time give good increment to the developed lateral soil pressure. The figure in 1.5D is more accurate and can be used in the design because it give greater value of lateral soil pressure which is more critical and also gives a significant large amount of lateral pile displacement.

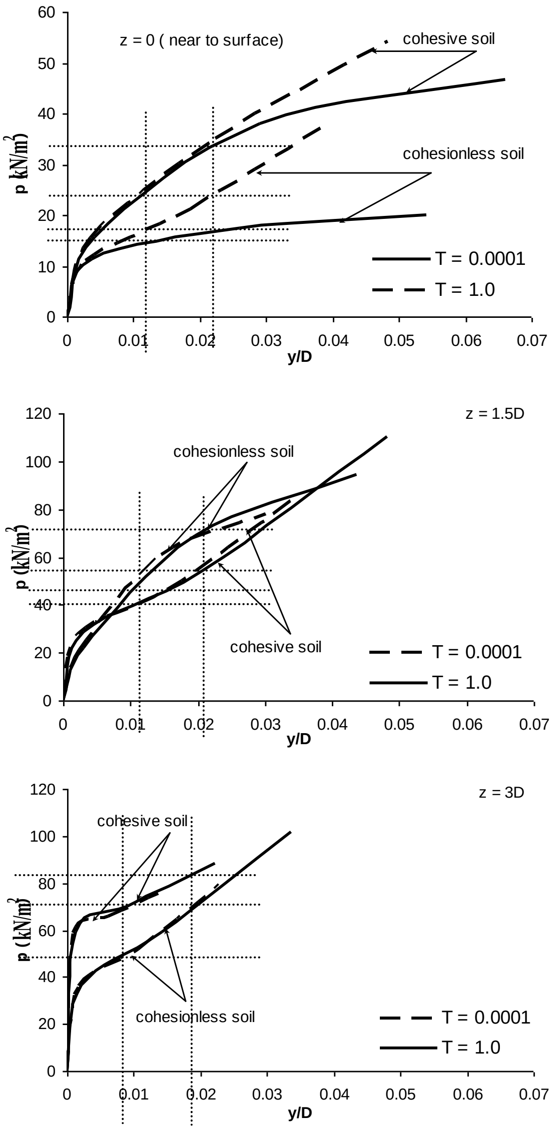

Figure 11. *p-y* curves predicted from the finite element simulation under the effect of time-dependent and with different depth below pile tip of pile embedded on two types of soil, L = 15m

6.0 Conclusions

The finite element approach coupled with consolidation equation is used to assess the lateral pile response when subjected to pure lateral load. Based on the results the following conclusions can be drawn:

The lateral pile response includes both lateral pile displacement and lateral soil pressure is affected by lateral load intensity and also change mainly by the long-time after applied load.

The pile in cohesionless soil is more resistant in the first stage of load (rapid load) and getting weaker with time after dissipation of pore water pressure (long term loading) compared with the pile embedded in cohesive soil.

The front lateral soil pressure distribution is changing mostly in the upper part of pile and reaches the maximum value at 1.25D this mean the final stage of loading. While in the first stage of low load intensity, the ultimate lateral load intensity occurred much close to the surface in both types soil. In addition, maximum negative lateral soil pressure occurred at the pile toe.

For the same amount of lateral deflection 10% and 20% of pile diameter, the result obtained from cohesionless soil gives less amounts than the results with cohesive soil. It is may be due to early collapse of surface soil mass in the case of cohesionless soil.

References

Abbas J M, Chik Z, Taha M R. 2008. Single pile simulation and analysis subjected to lateral load. *Electronic Journal of Geotechnical Engineering, SCOPUS*. 13 Bundle (E).: 1-15

Abbas J M, Chik Z, Taha M R, Shafiqu Q S M. 2009. Analysis of Time Dependent Laterally Loaded Pile in Clay. *Electronic Journal of Geotechnical Engineering*. 14 Bundle (N): 1-10.

Biot, M.A. 1941. General theory of three-dimensional consolidation. J. App. Phys., (12):155-164.

Broms B. B. 1964a . Lateral resistance of Piles in Cohesive Soils . *Journal of the Soil Mechanics and Foundations Division*, 90(2): 27-63.

Broms B. B. 1964b . Lateral resistance of Piles in Cohesionless Soils . *Journal of the Soil Mechanics and Foundations Division*, 90(3): 123-156.

Carter J.P, and Booker J.R. 1983. Consolidation of axi-symmetric bodies subjected to non-axi-symmetric loading. Inter. J. Num. Analy. Meth. Geomech ,7: 273-281.

Desai C. S. and Appel G. C. 1976 . 3-D Analysis of Laterally Loaded Structures . *Proceedings of the 2nd Int. Conf. Num. Methods in Geomechanics, Blacksburg, Virginia, ASCE*, (1).

Johnson, K., Lemcke, P., Karunasena, W., Sivakugan, N. 2006. Modelling the load – deformation response of deep foundation under oblique load. *Envir. Model. Soft.*, 21:1375-1380.

Karthigeyan, S., Ramakrishna, V. V. G. S. T. , and Rajagopal K. 2006. Influence of vertical load on the lateral response of piles in sand . *Comp. Geotech*., 33: 121-131.

Karthigeyan, S., Ramakrishna, V. V. G. S. T. , and Rajagopal K. 2007. Numerical Investigation of the Effect of Vertical Load on the Lateral Response of Piles . *J. Geotech. Geoenvir. Eng*. 133(5): 512-521.

Mroueh H. and Shahrour I. 2009. Numerical analysis of the response of battered piles to inclined pullout loads. *Int. J. Numer. Anal. Meth. Geomech*. 33:1277–1288

Muqtadir, A., and Desai, C. S. 1986. Three-dimensional analysis of a pile-group foundation. *Int. J. Num. Anal. Meth. Geomech*. 10: 41–58.

Poulos, H.G., Davis, E.H. 1980. *Pile Foundation Analysis and Design*. John Wiley & Sons, Inc, United States.

Potts, D. M., and Zdravkovic, L. 1999. *Finite element analysis in geotechnical engineering: theory*. Thomas Telford. Heron Quay, London.

Small, J. C., and Lui, H. L. S. 2008. Time-settlement behavior of piled raft foundation using infinite elements. *Comp. Geotech.* 35: 187-195.

Smith, I.M., and Griffiths, DV. 2004. *Programming Finite Element Method*. 4th Ed., John Wiley and Sons, Chisester, U.K.

Taiebat HT and Carter JP. 2001. A semi-analytical finite element method for three-dimensional consolidation analysis. *Comp. and Geotech*., 28: 55-78.

Trochanis, A.M. Bielak J., and Christiano, P. 1991. Threedimensional nonlinear study of piles. *J. Geotech. Engrg.*, 117(3): 429–447.